

# Novel Prodrug-Like Fusion Toxin with Protease-Sensitive Bioorthogonal PEGylation for Tumor Targeting

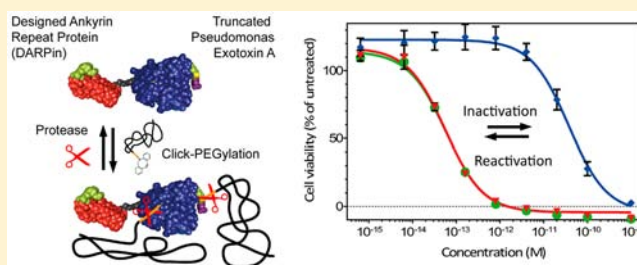
Nikolas Stefan,<sup>†,‡</sup> Martina Zimmermann,<sup>†</sup> Manuel Simon,<sup>†,‡</sup> Uwe Zangemeister-Wittke,<sup>\*,†,‡</sup> and Andreas Plückthun<sup>\*,†</sup>

<sup>†</sup>Department of Biochemistry, Winterthurerstrasse 190, University of Zurich, CH-8057 Zurich, Switzerland

<sup>‡</sup>Institute of Pharmacology, Friedbühlstrasse 49, University of Bern, CH-3010 Bern, Switzerland

## S Supporting Information

**ABSTRACT:** Highly potent biotoxins like *Pseudomonas* exotoxin A (ETA) are attractive payloads for tumor targeting. However, despite replacement of the natural cell-binding domain of ETA by tumor-selective antibodies or alternative binding proteins like designed ankyrin repeat proteins (DARPin) the therapeutic window of such fusion toxins is still limited by target-independent cellular uptake, resulting in toxicity in normal tissues. Furthermore, the strong immunogenicity of the bacterial toxin precludes repeated administration in most patients. Site-specific modification to convert ETA into a prodrug-like toxin which is reactivated specifically in the tumor, and at the same time has a longer circulation half-life and is less immunogenic, is therefore appealing. To engineer a prodrug-like fusion toxin consisting of the anti-EpCAM DARPIn Ec1 and a domain I-deleted variant of ETA (ETA<sup>ΔI</sup>), we used strain-promoted azide alkyne cycloaddition for bioorthogonal conjugation of linear or branched polyethylene glycol (PEG) polymers at defined positions within the toxin moiety. Reversibility of the shielding was provided by a designed peptide linker containing the cleavage site for the rhinovirus 3C model protease. We identified two distinct sites, one within the catalytic domain and one close to the C-terminal KDEL sequence of Ec1-ETA<sup>ΔI</sup>, simultaneous PEGylation of which resulted in up to 1000-fold lower cytotoxicity in EpCAM-positive tumor cells. Importantly, the potency of the fusion toxin was fully restored by proteolytic unveiling. Upon systemic administration in mice, PEGylated Ec1-ETA<sup>ΔI</sup> was much better tolerated than Ec1-ETA<sup>ΔI</sup>; it showed a longer circulation half-life and an almost 10-fold increased area under the curve (AUC). Our strategy of engineering prodrug-like fusion toxins by bioorthogonal veiling opens new possibilities for targeting tumors with more specificity and efficacy.



## ■ INTRODUCTION

Targeted delivery of cytotoxic payloads to tumor cells by antibodies and antibody fragments recognizing tumor-associated antigens has demonstrated clinical success in patients with hematological malignancies and solid tumors for which standard therapy had failed.<sup>1</sup> Recent progress in molecular oncology and tumor biology has identified surface markers which better discriminate between malignant and normal cells, and which can be used as receptors for tumor targeting also with highly cytotoxic antibody–drug conjugates. Due to its high potency, *Pseudomonas aeruginosa* exotoxin A (ETA) holds particularly great promise for this purpose.<sup>2,3</sup> However, even after replacement of its native cell binding domain by a tumor-selective ligand, unspecific target-independent cellular uptake leading to damage to normal vital tissues remains a major problem.

ETA belongs to the class of A-B toxins consisting of a receptor-binding domain, which enables cell entry, linked to an enzymatically active cytotoxin.<sup>2</sup> Upon receptor binding and endocytosis, pH-dependent proteolysis and reduction of a disulfide bond results in the release of the C-terminal cytotoxin subunit. By binding to the mammalian KDEL receptor with its

C-terminal sequence, the released fragment exploits retrograde transport from the endosome to the endoplasmic reticulum (ER) and subsequent translocation to the cytosol, where it ADP-ribosylates the eukaryotic elongation factor 2 (eEF2), resulting in cell death.

For tumor targeting, the receptor binding domain I of ETA has been replaced by tumor-specific binding molecules like antibody fragments recognizing tumor associated antigens or by cytokines.<sup>4</sup> We previously demonstrated that for tumor targeting with drug conjugates or fusion toxins, alternative non-IgG binding scaffolds such as designed ankyrin repeat proteins (DARPins) are more advantageous.<sup>5</sup> Derived from naturally occurring repeat proteins by consensus engineering, DARPins are composed of internal repeats for target binding which are flanked by N- and C-terminal capping repeats.<sup>6,7</sup> Their extraordinary thermodynamic stability facilitates engineering and results in high expression yields in *E. coli*, even for fusion proteins. Additional features like the lack of cysteines and compatibility with bioorthogonal click chemistry<sup>8</sup> distin-

Received: April 1, 2014

Published: October 28, 2014



guish DARPins for the generation of tailor-made protein therapeutics. Using DARPins recognizing the epithelial cell adhesion molecule (EpCAM) widely expressed in solid tumors<sup>9,10</sup> we demonstrated that ETA can be tailored for tumor targeting by rational protein engineering.<sup>11</sup> Nonetheless, even with the most tumor-specific delivery systems dose-limiting toxicity resulting from off-target effects on normal tissues remains as a major obstacle for clinical success.<sup>12–14</sup> In addition to choosing the right target on tumor cells, further engineering of ETA is therefore mandatory to increase its therapeutic window.

Several strategies were employed to even further increase the cytotoxic potency of ETA in mammalian cells, such as replacement of the native C-terminal residues, REDLK, with the canonical eukaryotic ER-retention signal KDEL and, more recently, the generation of ETA mutants resisting endolysosomal degradation.<sup>15–17</sup> Furthermore, efforts were made to reduce the immunogenicity of the toxin, for instance, through elimination of immunodominant B- and T-cell epitopes by introducing point mutations or deletions.<sup>18–20</sup> Alternatively, by chemical modification with polyethylene glycol (PEG),<sup>21,22</sup> ETA fusion toxins with reduced immunogenicity and extended serum half-life were generated.<sup>23,24</sup> We hypothesized that such polymer coating of ETA deserves attention also for prodrug design, as it may compromise toxin function by steric hindrance of the intoxication process with the potential to reduce off-target toxicity upon systemic administration. However, the polymer then has to be attached to a carefully chosen place, such as within the toxin domain, and veiling would have to be reversible and be abrogated by proteases specifically produced in the tumor to unleash the toxin's full cytotoxic potential.

Traditional chemistries for PEGylation use either the thiol groups of cysteines or the primary amino groups of lysines as conjugation sites. However, since fusion toxins used for tumor targeting (such as ETA) usually contain several of these amino acids, this inevitably results in positional isomers and attachment of more than one PEG, which may negatively affect manufacture and cytotoxic activity.<sup>25–27</sup> Recently, we described the use of strain-promoted azide alkyne cycloaddition (also termed Cu-free click chemistry) enabling double functionalization of DARPins.<sup>8</sup> The same chemistry was recently used also for site-specific N-terminal PEGylation of a fusion toxin consisting of the anti-EpCAM DARPin Ec1 and a domain I-truncated form of exotoxin A (here denoted ETA").<sup>11</sup> The increased hydrodynamic radius improved the pharmacokinetic performance, which translated into longer lasting antitumor effects at lower doses. The bulky polymer (attached at the N-terminus of the DARPin) slightly decreased the cytotoxicity of the toxin *in vitro*, probably due to dynamic blocking effects. However, we found that if a protease-sensitive linker was used for conjugation, the toxicity could be fully restored by proteolytic removal of PEG.<sup>11</sup> The possibility to orthogonally link PEG polymers via a designed linker containing the cleavage site of a tumor-specific protease thus holds promise for engineering prodrug-like fusion toxins with better safety and efficacy profiles.

Here, we employed bioorthogonal strain-promoted click chemistry for PEGylation of a DARPin-ETA" fusion toxin, remote from the EpCAM-binding DARPin domain, at distinct positions within the catalytic domain III of the toxin and close to the C-terminal KDEL sequence. We identified arrangements where maximum inhibition of cytotoxicity could be achieved using branched and linear PEG polymers. As a proof of concept

for prodrug design, we used a rhinovirus 3C protease-sensitive linker to demonstrate under experimentally defined conditions *in vitro* that toxin veiling and unveiling by proteases holds promise for increasing the specificity of ETA" fusion toxins for cancer therapy. Furthermore, we demonstrate that PEGylation within the toxin moiety reduced systemic toxicity *in vivo*, despite an almost 10-fold increased AUC.

## RESULTS

**Generation of DARPin-ETA" Fusion-Toxins Containing a Unique Clickable Residue at Distinct Positions.** To test the hypothesis that the fusion toxin Ec1-ETA", consisting of the anti-EpCAM DARPin Ec1<sup>28</sup> linked to domain I-truncated *Pseudomonas* exotoxin A, can be converted into a prodrug with decreased systemic toxicity, it was conjugated with a bulky PEG polymer using a protease-sensitive linkage. To facilitate site-specific modification, toxin mutants containing a unique azidohomoalanine (Aha) residue at distinct positions for bioorthogonal click chemistry were generated. In a first step, the amino acid at position 2 was changed from Arg to Ala (N-terminal sequence MAGSH<sub>6</sub>), leading to quantitative proteolytic removal of the initiator Aha in Met-free Aha-supplemented medium by *E. coli* (Supporting Information Figure S1).<sup>29</sup> Due to the lack of additional ATG codons in the Ec1 DARPin, a unique Aha for the click reaction can in principle be introduced at any desired position in the protein sequence.

Examination of the crystal structure (PDB: 2ZIT)<sup>30</sup> of the catalytic domain of ETA in complex with the cofactor NAD<sup>+</sup> and its substrate eEF2 identified 14 surface-exposed residues in the catalytic domain close to the active site or the interaction surface with eEF2, but not in direct contact with substrate or cofactor (Figure 1). Based on this information, we generated

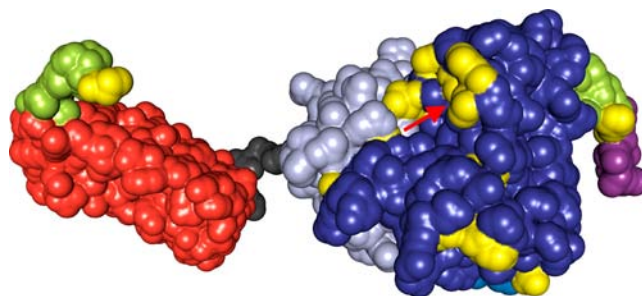


**Figure 1.** Model of the DARPin-toxin construct built on the basis of the X-ray structures of a consensus DARPin (PDB: 2QYJ) and full-length *Pseudomonas* exotoxin A (ETA, PDB: 1IKQ) using InsightII (Accelrys) and the ROSETTA suite of programs. The figure shows the DARPin (red) and the truncated ETA (ETA", different shades of blue) connected by a flexible linker (dark gray). The N-terminal MRGS-His<sub>6</sub>-tag (green), the C-terminal His<sub>6</sub> (green), and the KDEL ER-retention sequence (purple) are indicated. Positions mutated to Aha are indicated in yellow; the active site is indicated by a red arrow. The figure was generated using the program PyMol (DeLano Scientific LLC).

Ec1-ETA" mutants containing a unique internal Aha by changing the coding sequences of the selected positions to ATG using site-directed mutagenesis (Supporting Information Table S1). In addition, we generated a mutant containing a single Aha close to the C-terminal KDEL motif (AhaKDEL) and a mutant with an Aha replacing the active site residue Glu-553 (S53Aha).

The various fusion toxins containing Aha at distinct positions were expressed in the methionine-auxotrophic *E. coli* strain B834(DE3) using a medium exchange strategy for metabolic introduction of Aha.<sup>8,11</sup> All variants expressed well and yielded between 5.7 and 8.9 mg/L soluble Aha-containing proteins after IMAC purification. SDS-PAGE revealed the expected size of 59 kDa (data not shown).

**Cytotoxicity of Fusion Toxin Mutants.** To investigate whether the mutations by themselves (i.e., without coupling to PEG) negatively affected toxin activity, EpCAM-positive HT29 cells were incubated with serial dilutions of the different fusion toxins for 72 h and viability was measured in XTT assays (Figure 2). The corresponding IC<sub>50</sub> values are summarized in

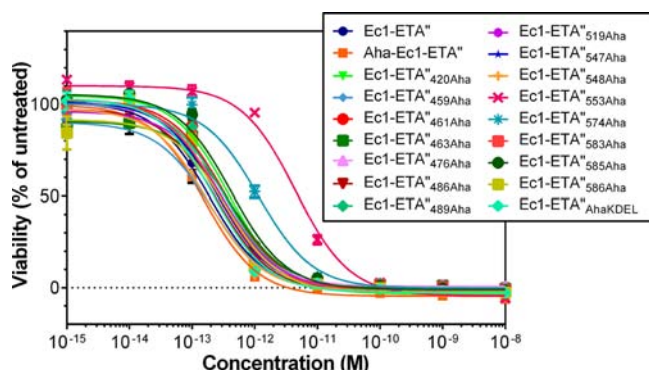


**Figure 2.** Cytotoxicity of Ec1-ETA'' and single Aha mutants derived thereof. Serial dilutions of the proteins were added to EpCAM-positive HT29 cells and viability was determined in XTT assays. Data are presented as mean  $\pm$  SD.

Supporting Information Table S1. The cytotoxicity of most mutants remained unchanged or decreased only slightly (max. 2.3-fold lower potency) compared to wild-type Ec1-ETA''. A more pronounced loss of toxicity was measured only for D574Aha (6.1-fold) and, as expected, for the active-site mutant E553Aha (23.8-fold). This demonstrates that most of the single mutations were well tolerated by the toxin and are hence suitable for bioorthogonal modification.

**Synthesis of PEG-3C-DBCO for Click Chemistry.** To enable reversible PEGylation using click chemistry, a linker peptide containing a recognition motif of the model protease 3C from rhinovirus was engineered, as this protease has high sequence specificity. DBCO-maleimide was reacted with the C-terminal cysteine of the peptide SDSLEVLFIQGPC (termed 3C for simplicity), where the vertical divider indicates the cleaved peptide bond. This DBCO-containing peptide was then conjugated at the N-terminal amino group to mPEG-succinimidyl valerate 20 kDa (PEG<sub>20 kDa</sub>-SVA) to produce PEG-3C-DBCO. Unreacted DBCO-maleimide and 3C-DBCO were removed on a desalting column, and excess PEG<sub>20 kDa</sub>-SVA was separated from the product PEG-3C-DBCO by anion exchange chromatography (Figure 3A). The main species (peak 3) absorbed at 309 nm, which is characteristic for DBCO. Analysis by native PAGE and PEG-staining with barium iodide<sup>31</sup> revealed a single band which migrated more rapidly on the gel than excess PEG<sub>20 kDa</sub>-SVA (peak 1), as expected for a PEGylated peptide containing two negatively charged amino acids (Figure 3B). Peak 5, which absorbed at 309 nm although it did not contain PEG, most likely represented unreacted 3C-DBCO. Removal of this side product was crucial, as it would compete with PEG-3C-DBCO in the click reaction. The PEG-

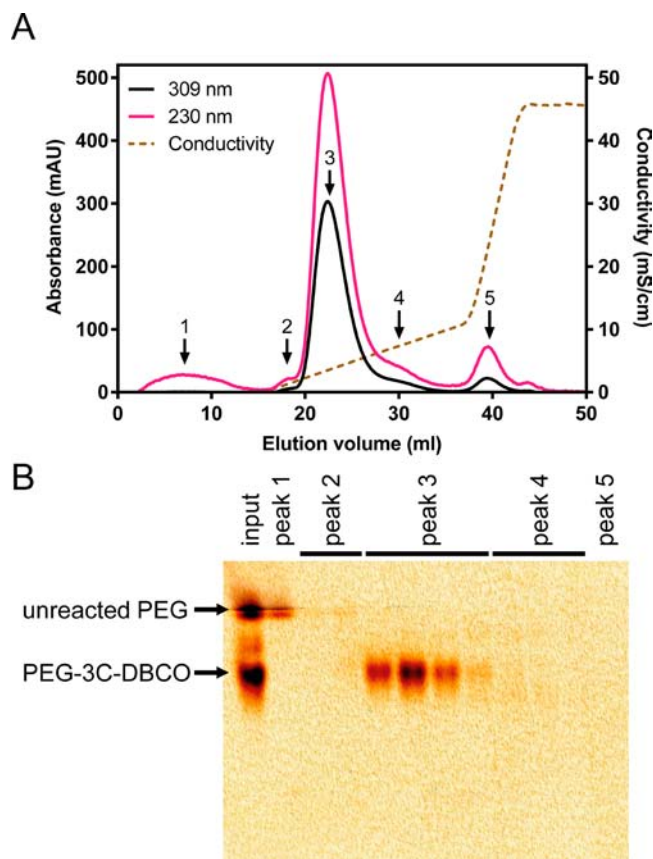


**Figure 3.** (A) Purification of PEG-3C-DBCO by anion exchange chromatography. (B) Analysis by native PAGE followed by staining for PEG with barium iodide.

3C-DBCO-containing fractions were pooled, desalted, quantified by measuring the absorption at 309 nm, lyophilized, and stored at  $-20^{\circ}\text{C}$ . The final yield of PEG-3C-DBCO was 60%. This 3C protease-sensitive PEGylation reagent was now ready to use for site-specific conjugation to the Ec1-ETA'' mutants.

#### Reversible Click-PEGylation of Fusion Toxin Mutants.

Nine "clickable" Ec1-ETA'' mutants were selected for conjugation with a linear PEG-3C-DBCO to generate fusion toxins reversibly PEGylated at Aha at distinct positions (see above). Incubation of the proteins with a 3-fold molar excess of PEG-3C-DBCO resulted in quantitative PEGylation. The PEGylated proteins were separated from the reactants by anion exchange chromatography followed by preparative gel filtration. Analysis of the final products by SDS-PAGE stained with Coomassie and barium iodide revealed that the position of PEG-conjugation changed the running behavior (Figure 4A). Conjugation with the PEG polymer in the middle of the unfolded protein chain produces a branched chain, and it would be expected that its friction with the polyacrylamide matrix depends on the position of the branch point. On the other hand, during analytical gel filtration, where the protein remains folded, all PEGylated Ec1-ETA'' variants eluted at identical volumes, providing evidence for site-specific mono-PEGylation (Figure 5).

To demonstrate that the conjugated PEG polymer can be quantitatively removed from the Ec1-ETA'' mutants, the PEGylated proteins were incubated with 3C protease for 2 h on ice. As shown in Figure 4B, this resulted in quantitative proteolysis within the linker peptide as shown by SDS-PAGE



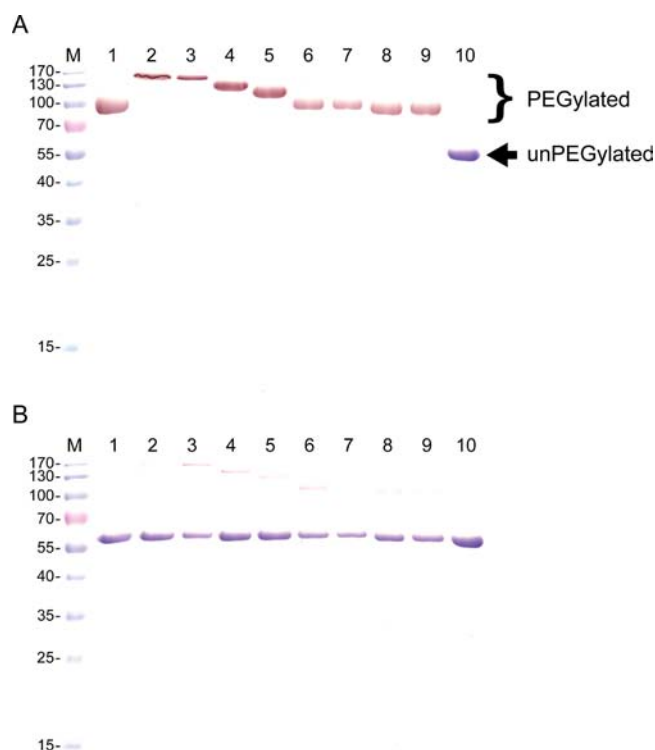


**Figure 4.** SDS-PAGE analysis of PEGylated Ec1-ETA<sup>''</sup> variants before (A) and after (B) dePEGylation with 3C protease for 2 h on ice on a 12% polyacrylamide gel stained with Coomassie and barium iodide: lane M, molecular weight marker (kDa); lane 1, PEG-3C-Ec1-ETA<sup>''</sup>; lane 2, Ec1-ETA<sup>''</sup><sub>459Aha</sub>-3C-PEG; lane 3, Ec1-ETA<sup>''</sup><sub>461Aha</sub>-3C-PEG; lane 4, Ec1-ETA<sup>''</sup><sub>486Aha</sub>-3C-PEG; lane 5, Ec1-ETA<sup>''</sup><sub>489Aha</sub>-3C-PEG; lane 6, Ec1-ETA<sup>''</sup><sub>553Aha</sub>-3C-PEG; lane 7, Ec1-ETA<sup>''</sup><sub>574Aha</sub>-3C-PEG; lane 8, Ec1-ETA<sup>''</sup><sub>586Aha</sub>-3C-PEG; lane 9, Ec1-ETA<sup>''</sup><sub>AhaKDEL</sub>-3C-PEG; lane 10, Ec1-ETA<sup>''</sup>.

stained for protein and PEG. The bands of all Ec1-ETA<sup>''</sup> mutants shifted back to their original molecular weight of 59 kDa and became undetectable by barium iodide, confirming quantitative removal of PEG. Thus, using bioorthogonal click chemistry and a designed protease-sensitive PEG-linker peptide, we were able to generate reversibly PEGylated fusion toxins.

**Cytotoxicity of PEGylated Fusion Toxin Mutants.** To determine whether reversible PEGylation of the fusion toxin at the distinct positions decreased its cytotoxicity, IC<sub>50</sub> values were determined in XTT assays as described above. Furthermore, we tested whether proteolytic removal of the polymer restored the original potency to that of wild-type Ec1-ETA<sup>''</sup> on EpCAM-positive tumor cells. Compared with the N-terminally modified PEG-3C-Ec1-ETA<sup>''</sup>, all PEGylated Ec1-ETA<sup>''</sup> mutants showed further decreased cytotoxicity (Supporting Information Table S2). Importantly, proteolytic removal of the polymer fully restored the toxin's potency in the case of the mutants 459Aha, 461Aha, 486Aha, 489Aha, and the N-terminally PEGylated toxin, whereas dePEGylation only partly restored the activity of mutants 553Aha, 574Aha, 586Aha, and AhaKDEL. It should be noted that dePEGylation leaves a small stump of a tripeptide (GPC-maleimide-DBCO) linked to the protein.

As a measure for the difference in activity of PEGylated vs. dePEGylated fusion toxin and thus the quality of the prodrug

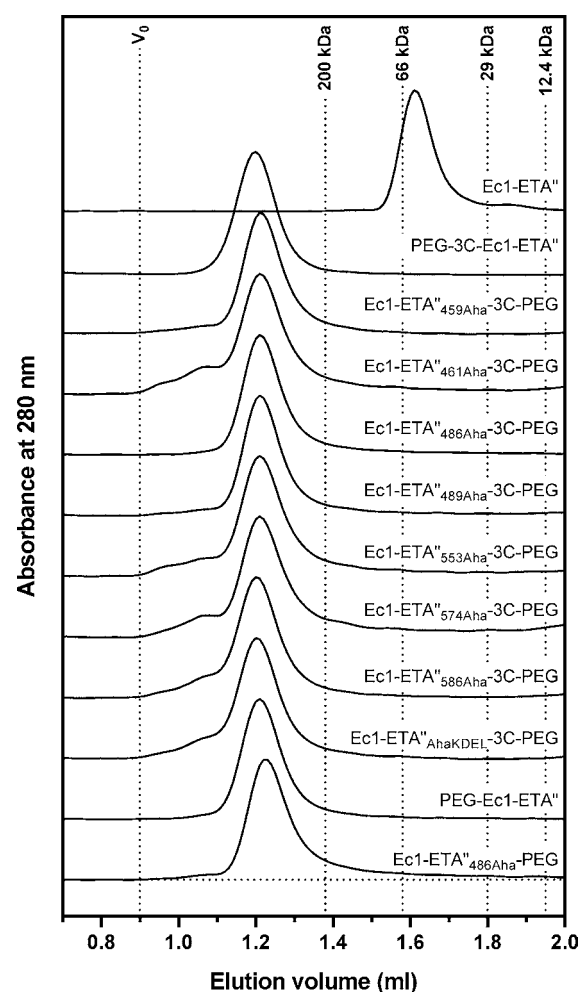


**Figure 5.** Analytical gel filtration of unmodified and reversibly PEGylated Ec1-ETA<sup>''</sup> mutants (Superdex 200 PC3.2). The molecular mass standards  $\beta$ -amylase (200 kDa), BSA (66 kDa), carbonic anhydrase (29 kDa), and cytochrome *c* (12.4 kDa) as well as the exclusion volume ( $V_0$ ) are indicated.

design, a toxin reactivation index was defined (eq 1), which indicates the protective function of the PEGylation.

$$\text{Reactivation index} = \frac{\text{IC}_{50} \text{ PEGylated mutant}}{\text{IC}_{50} \text{ dePEGylated mutant}} \quad (1)$$

With an index >12.1, the domain III mutants 459Aha, 486Aha, 489Aha, and AhaKDEL were found to behave better than the N-terminally PEGylated fusion toxin, whereas the mutants 461Aha, 553Aha, 574Aha, and 586Aha performed worse (Supporting Information Table S2). To have a large reactivation index, a mutant must show a well decreased cytotoxicity by the PEG polymer, and after dePEGylation, the effect of the remaining stump on toxin activity should be negligible.

The PEGylated fusion toxin with the highest reactivation index and thus the most promising prodrug-like construct was Ec1-ETA<sup>''</sup><sub>486Aha</sub>. Here, introduction of Aha alone did not negatively affect cytotoxicity, whereas PEGylation led to a 30-fold increase in the IC<sub>50</sub> (Supporting Information Table S2). Proteolytic dePEGylation fully restored the cytotoxicity to that of wild-type Ec1-ETA<sup>''</sup>. Furthermore, this PEGylated fusion toxin mutant showed monomeric behavior in gel filtration in contrast to the other constructs which showed some signs of

dimerization or even higher order oligomerization (Figure 5). Ec1-ETA<sup>486Aha</sup>-3C-PEG was therefore selected for further characterization.

Testing of Ec1-ETA<sup>486Aha</sup> on additional EpCAM-positive tumor cell lines also revealed increased reactivation indices compared to N-terminally PEGylated fusion toxin with MCF7, A431, MKN-45, and SKOV3, but not with SKBR3 cells (Table 1). To exclude the possibility that the peptide linker containing

**Table 1. Reactivation Indices of Reversibly PEGylated Fusion Toxins with and without Ec1 as Competitor Determined on Various Tumor Cell Lines**

|   | reactivation index <sup>a</sup> |       |      |        |       |       |
|---|---------------------------------|-------|------|--------|-------|-------|
|   | HT29                            | MCF-7 | A431 | MKN-45 | SKOV3 | SKBR3 |
| PEG-3C-Ec1-ETA <sup>486Aha</sup>        | 12.6                            | 4.8   | 7.6  | 10.1   | 5.4   | 4.4   |
| Ec1 + PEG-3C-Ec1-ETA <sup>486Aha</sup>  | 10.9                            | 7.1   | 4.8  | 11.7   | 3.2   | 3.4   |
| Ec1-ETA <sup>486Aha</sup> -3C-PEG       | 20.6                            | 8.1   | 30.2 | 18.9   | 9.5   | 3.0   |
| Ec1 + Ec1-ETA <sup>486Aha</sup> -3C-PEG | 28.4                            | 18.8  | 25.6 | 29.6   | 13.6  | 10.7  |

<sup>a</sup>The reactivation index is defined in eq 1.

the 3C protease site was cleaved by irrelevant cellular proteases leading to premature reactivation of the toxin, we also conjugated Aha-Ec1-ETA<sup>486Aha</sup> and Ec1-ETA<sup>486Aha</sup> with a non-cleavable PEG<sub>20 kDa</sub>-DBCO construct as control. Irreversible PEGylation inhibited cytotoxicity with almost identical efficiency compared to the 3C-cleavable variants (Supporting Information Table S3), thus confirming the high stability of the 3C-sensitive linker construct in the absence of the specific protease.

Moreover, to simulate unspecific toxin uptake by EpCAM-negative cells, competition with free Ec1 DARPin was used to block EpCAM binding and endocytosis. Under these conditions, the reactivation index of Ec1-ETA<sup>486Aha</sup> increased with most cell lines including SKBR3, but not with A431 (Supporting Information Table S3), and similar results were obtained with the unspecific cytotoxicity of fusion toxins made with the methionine-free control DARPin Off7ΔM. This confirms that inhibition of toxin activity by site-specific PEGylation was independent of EpCAM binding (Supporting Information Tables S3 and S4), and most likely affects steps in the retrograde transport to the ER and/or the actual transport step to the cytoplasm, in addition to the enzymatic reaction itself (see below). Thus, with Ec1-ETA<sup>486Aha</sup> we identified a fusion toxin candidate with the most promising properties for prodrug engineering by reversible PEGylation, which was selected for further characterization.

**Inhibition of Translation by PEGylated Ec1-ETA<sup>486Aha</sup>.** To investigate whether PEGylation of Ec1-ETA<sup>486Aha</sup> directly affects the ADP-ribosylation activity of the toxin, *in vitro* translation reactions were performed in the presence of eEF2 and serial dilutions of fusion toxin. The amount of translated *Renilla* luciferase was quantified and used to calculate IC<sub>50</sub> values (Supporting Information Figure S2). The Aha mutation at position 486 alone only marginally decreased toxin activity 2.1-fold, which was further decreased 2-fold by PEGylation. When the cleavable linker construct was used, inhibition was fully reversed by removal of the polymer. In contrast, not unexpectedly, N-terminal PEGylation did not affect toxin activity in the assays. This indicates that the reduced enzymatic

activity of the toxin contributes to the decreased cytotoxicity of Ec1-ETA<sup>486Aha</sup> upon bioorthogonal protease-sensitive PEGylation. However, the effect on the enzymatic activity is comparatively small, such that PEGylation can be assumed to mainly impair retrograde transport and/or uptake into the cytoplasm (see below).

**Binding Affinity of PEGylated Ec1-ETA<sup>486Aha</sup> Mutants.** The interaction of Ec1-ETA<sup>486Aha</sup>-3C-PEG with its target EpCAM was examined by surface plasmon resonance measurements in comparison with the N-terminally PEGylated and unmodified Ec1-ETA<sup>486Aha</sup> fusion toxins (Table 2, Supporting Information

**Table 2. Affinity of PEGylated Fusion Toxins Determined by Surface Plasmon Resonance Measurements**

| protein                                   | $k_{on}$<br>(M <sup>-1</sup> s <sup>-1</sup> ) | $k_{off}$<br>(s <sup>-1</sup> ) | $K_D$<br>(M)          | $R_{max}$<br>(RU) |
|---|--|---------------------------------|-----------------------|-------------------|
| Ec1-ETA <sup>486Aha</sup>                 | $1.7 \times 10^4$                              | $5.3 \times 10^{-6}$            | $3.2 \times 10^{-10}$ | 716               |
| PEG-3C-Ec1-ETA <sup>486Aha</sup>          | $8.0 \times 10^3$                              | $7.2 \times 10^{-6}$            | $8.9 \times 10^{-10}$ | 322               |
| Ec1-ETA <sup>486Aha</sup> -3C-PEG         | $1.8 \times 10^4$                              | $5.7 \times 10^{-6}$            | $3.2 \times 10^{-10}$ | 336               |
| Ec1-ETA <sup>486Aha</sup> -3C-Y-PEG       | $1.9 \times 10^4$                              | $6.3 \times 10^{-6}$            | $3.3 \times 10^{-10}$ | 273               |
| Ec1-ETA <sup>486Aha</sup> -AhaKDEL-3C-PEG | $8.8 \times 10^3$                              | $6.0 \times 10^{-6}$            | $6.8 \times 10^{-10}$ | 295               |

Figure S3). As reported previously,<sup>11</sup> we found that N-terminal PEGylation of Ec1-ETA<sup>486Aha</sup> resulted in a lower association rate constant  $k_{on}$  and a lower maximum of bound analyte ( $R_{max}$ ), due to intra- and intermolecular blocking,<sup>32</sup> respectively. Although some perturbed binding was also measured for Ec1-ETA<sup>486Aha</sup>-3C-PEG (Table 2), the effect was less than with the N-terminally modified fusion toxin, and  $k_{on}$  values similar to unPEGylated toxin were observed. Also, attachment of a branched 40 kDa PEG at positions 486 (see below) (abbreviated Y-PET) did not negatively affect the association rate, but resulted in stronger intermolecular blocking (i.e., lower levels of binding at saturation). Dual-PEGylation at position 486 and near the C-terminal KDEL peptide (see below) slightly decreased the  $k_{on}$  values to the level observed for N-terminally PEGylated toxin. This rules out that the decreased cytotoxicity of this fusion toxin compared to the N-terminally PEGylated variant was due to impaired binding to EpCAM. On the contrary, EpCAM binding appeared less impaired when PEG was attached to the toxin, since intramolecular blocking (i.e., lowering of the on-rate) was less pronounced for Ec1-ETA<sup>486Aha</sup>-3C-PEG.

**Enhanced Inhibition of Cytotoxicity by Dual-PEGylation.** To further improve our prodrug design and achieve an even more pronounced reversible inhibition of cytotoxicity, two further PEGylation strategies were explored using the Ec1-ETA<sup>486Aha</sup> fusion toxin mutant: (1) conjugation of a branched 40 kDa PEG (termed Y-PEG for simplicity) and (2) conjugation of two linear 20 kDa PEG polymers at two distinct sites. For strategy (1), a branched Y-PEG-3C-DBCO construct was synthesized and purified analogously to linear PEG-3C-DBCO and coupled to Ec1-ETA<sup>486Aha</sup> or the Off7ΔM-ETA<sup>486Aha</sup> control to obtain Ec1-ETA<sup>486Aha</sup>-3C-Y-PEG and Off7ΔM-ETA<sup>486Aha</sup>-3C-Y-PEG. For strategy (2), a double mutant with an additional Aha residue next to the C-terminal KDEL peptide (Ec1-ETA<sup>486Aha</sup>-AhaKDEL) was produced and reacted with a 4-fold excess of linear PEG-3C-DBCO. Both coupling reactions went nearly to completion with almost no unPEGylated protein remaining and only small amounts of

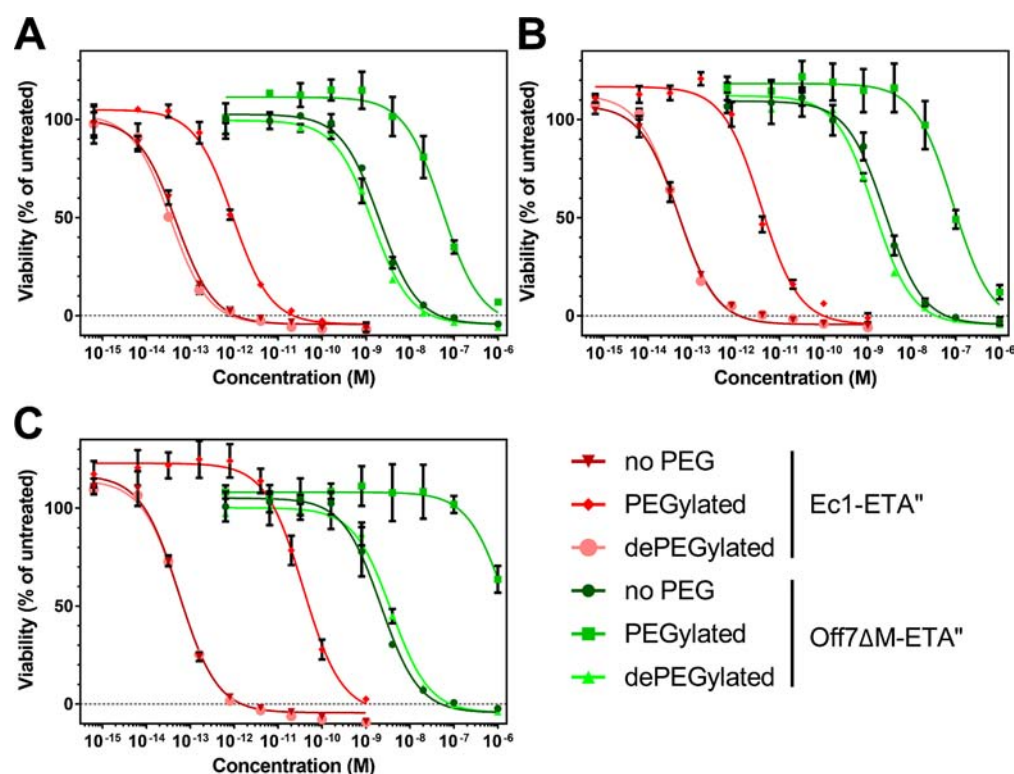


**Figure 6.** EpCAM-dependent (red, using EpCAM-specific DARPin Ec1) and EpCAM-independent (green, using control DARPin Off7) cytotoxicity of unPEGylated, PEGylated, and proteolytically dePEGylated DARPin-ETA". Protein toxins were site-specifically conjugated with linear 20 kDa PEG (A, DARPin-ETA''<sub>486Aha</sub>-3C-PEG), branched 40 kDa PEG (B, DARPin-ETA''<sub>486Aha</sub>-3C-Y-PEG), or two linear 20 kDa PEGs (C, DARPin-ETA''<sub>486Aha</sub>-AhaKDEL-3C-PEG). For dePEGylation, proteins were incubated with 3C protease. Serial dilutions of the proteins were added to EpCAM-positive HT29 cells and viability was measured in XTT assays. Data are presented as mean  $\pm$  SD. PEG: polyethylene glycol.

mono-PEGylated side-products in reaction (2), which was readily removed by the purification procedure described above.

As measured in cell viability assays with HT29 cells, both PEGylation strategies indeed further decreased the cytotoxicity of ETA" compared to PEGylation with only a single linear polymer (Figure 6). Whereas conjugation of a single Y-PEG resulted in an 80-fold inhibition, double-modification with two linear PEG polymers was even more effective and resulted in a more than 600-fold higher IC<sub>50</sub> (Table 3 and Supporting Information Table S4). Both fusion toxin variants were fully reactivated upon proteolytic dePEGylation. The strong inhibition of toxin activity as a result of dual-PEGylation was confirmed on other EpCAM-positive tumor cell lines where

Ec1-ETA''<sub>486Aha</sub>-AhaKDEL-3C-PEG also exhibited 15- to 25-fold greater reactivation indices compared to mono-PEGylated Ec1-ETA''<sub>486Aha</sub>-3C-PEG.

Similarly, dual-PEGylation also reversibly decreased the unspecific cytotoxicity of the control fusion toxin Off7ΔM-ETA" for which overall reactivation indices up to 750-fold were calculated (Table 3). Thus, conjugation of two linear 20 kDa PEG polymers at position 486 and a site upstream of the C-terminal KDEL peptide was identified as most optimal for engineering a prodrug-like fusion toxin with enhanced tumor specificity. The remarkably strong effect of PEGylation on the cytotoxicity of the nontargeted control suggests that PEG blocks the unspecific toxin uptake by pinocytosis and/or its subsequent transfer to the cytosol, and this may be even more crucial for this prodrug effect than PEG inhibiting the enzymatic activity itself.

**In Vivo Pharmacokinetics and Toxicity upon Systemic Administration in Mice.** In line with earlier studies using irreversibly mono-PEGylated fusion toxins,<sup>11</sup> the circulation half-life of Ec1-ETA''<sub>486Aha</sub>-AhaKDEL-3C-PEG was markedly increased compared to the unPEGylated protein (82 and 7.5 min, respectively), resulting in an almost 10-fold increased AUC (Supporting Information Figure S4). To investigate the effect of toxin inhibition by PEGylation on systemic toxicity, a single dose of Ec1-ETA''<sub>486Aha</sub>-AhaKDEL-3C-PEG or Ec1-ETA" was administered *i.v.* to C57BL/6 mice (3 to 5 per group). Body weight was monitored for 3 days after injection before sacrificing the animals to assess liver toxicity by quantification of alanine aminotransferase (ALT) and aspartate aminotransferase (AST) activity in serum samples. As shown in

**Table 3.** Reactivation Indices of Ec1-ETA" and Off7ΔM-ETA" Modified with One or Two Linear PEGs or Branched PEG Determined on Various Tumor Cell Lines

|  | reactivation index <sup>a</sup> |             |             |             |
|--|---------------------------------|-------------|-------------|-------------|
|  | HT29                            | MCF-7       | MDA-MB-468  | MDA-MB-231  |
| Ec1-ETA'' <sub>486Aha</sub> -3C-PEG            | 26.0                            | 6.9         | 12.0        | 49.5        |
| Off7ΔM-ETA'' <sub>486Aha</sub> -3C-PEG         | 39.0                            | 35.6        | 55.6        | 37.4        |
| Ec1-ETA'' <sub>486Aha</sub> -3C-Y-PEG          | 80.5                            | <i>n.d.</i> | <i>n.d.</i> | <i>n.d.</i> |
| Off7ΔM-ETA'' <sub>486Aha</sub> -3C-Y-PEG       | 62.1                            | <i>n.d.</i> | <i>n.d.</i> | <i>n.d.</i> |
| Ec1-ETA'' <sub>486Aha</sub> -AhaKDEL-3C-PEG    | 637.0                           | 110.8       | 185.6       | 1221.4      |
| Off7ΔM-ETA'' <sub>486Aha</sub> -AhaKDEL-3C-PEG | 412.6                           | 650.3       | 750.9       | 143.1       |

<sup>a</sup>The reactivation index is defined in eq 1. *n.d.* = not determined.

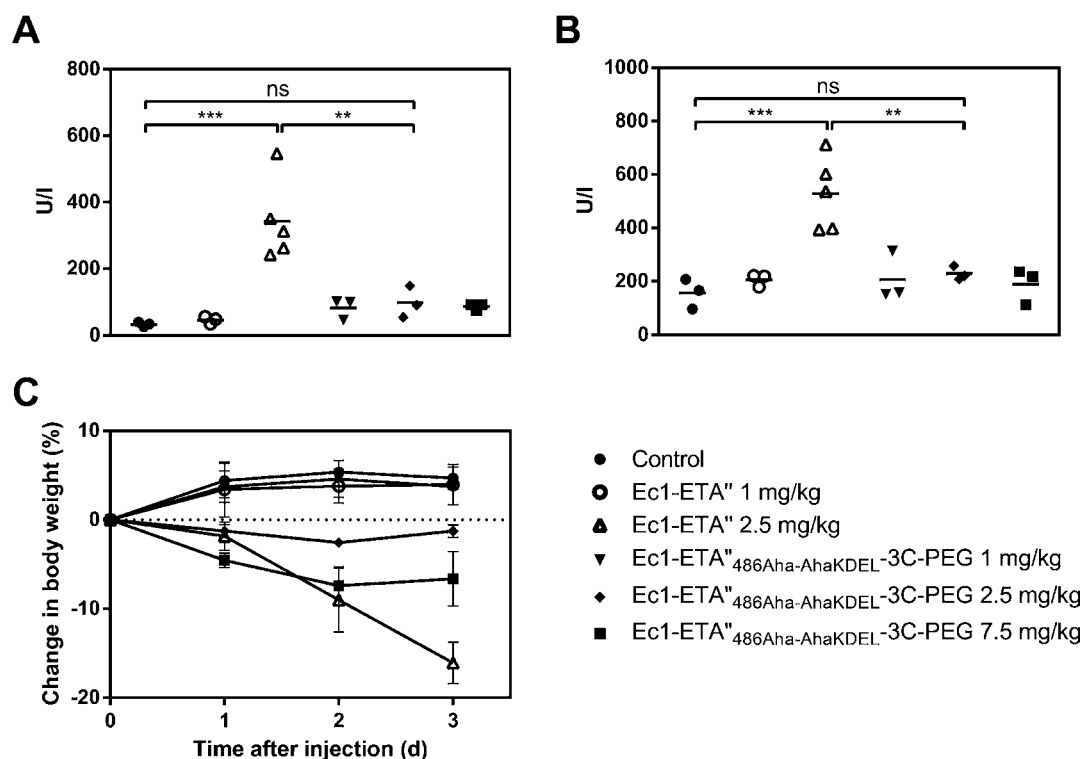


**Figure 7.** *In vivo* toxicity of unPEGylated and PEGylated DARPin-ETA" in C57BL/6 mice. Toxicity of a single dose of Ec1-ETA" and Ec1-ETA" 486Aha-AhaKDEL-3C-PEG injected *i.v.* was assessed by quantification of ALT (A) and AST (B) activity in serum samples as well as by monitoring body weight (C). For each group, 3 to 5 mice were analyzed. Statistical analysis was performed using one-way ANOVA with Sidak's multiple comparison test; ns: not significant ( $p \geq 0.05$ ), \*\*  $p < 0.01$ , \*\*\*  $p < 0.001$ .

Figure 7C, a single dose of 2.5 mg/kg Ec1-ETA" resulted in body weight loss exceeding 15% on day 3 so that the animals had to be euthanized. In contrast, the same dose of Ec1-ETA" 486Aha-AhaKDEL-3C-PEG was well tolerated with a maximum weight loss of only 2.6% on day 2 and mice started to regain weight on day 3. Moreover, mice lost only 7.4% of body weight on day two after administration of 7.5 mg/kg of the PEGylated fusion toxin and regained weight on day 3. Consistent with the considerable loss of body weight after administration of 2.5 mg/kg Ec1-ETA", this treatment also resulted in significantly higher levels of ALT and AST after 72 h, compared to both doses of the prodrug Ec1-ETA" 486Aha-AhaKDEL-3C-PEG (Figure 7A,B). Altogether, our data demonstrate that reversible toxin inactivation by simultaneous PEGylation at position 486 and upstream of the C-terminal KDEL motif effectively diminished systemic toxicity, thereby allowing higher doses of the prodrug to be administered, despite a longer circulation half-life and thus prolonged drug exposure of the animals.

## DISCUSSION

The potential of highly potent fusion toxins for tumor targeting is limited by unspecific cellular uptake in normal tissues, which is independent of receptor expression and may occur through pinocytosis. This implies that every such toxin can cause side effects by nontargeted damage which inevitably decreases the therapeutic window. Therefore, apart from receptor-specific targeting, additional mechanisms must be introduced into the toxin to establish a second layer of specificity. Here, we investigated a prodrug concept which involves veiling with a bulky polymer to decrease toxin activity, followed by reactivation under conditions specifically found in the tumor microenvironment. This design offers the possibility to keep

the toxin's destructive potential in check before tumor localization has occurred.

Conjugation of PEG polymers to anticancer agents like small molecule drugs, peptides, and proteins by stable linkage is an established technology to improve their pharmacokinetic performance and thus efficacy.<sup>21</sup> The large hydrodynamic radius of PEG prevents rapid renal clearance leading to increased circulation half-lives, and it provides steric shielding and stealth properties, thereby reducing physical degradation and immune recognition.<sup>22</sup> On the other hand, these desirable properties may come at the price of decreased efficacy due to steric hindrance of the bulky polymer with biological functions like cell binding, internalization, and access to the intracellular target.<sup>26,32</sup> These considerations hold particularly true for ETA fusion toxins. Although covalent PEGylation, either randomly at lysine residues<sup>33</sup> or site-specifically at unpaired cysteines introduced into the protein by mutation,<sup>23,24</sup> was shown to extend the terminal circulation half-life of the fusion toxin, at the same time it decreased cytotoxicity and therapeutic efficacy. This shortcoming might be a consequence of the unselective nature of the modification and might result in incorrectly folded and functionally impaired proteins. We recently reported on a fusion toxin consisting of an anti-EpCAM DARPin and domain I-truncated ETA (ETA") which was N-terminally PEGylated using bioorthogonal Cu-free click chemistry known as strain-promoted azide alkyne cycloaddition.<sup>11</sup> This site-specific PEGylation, which only minimally interferes with binding but greatly increases the half-life, indeed increased the antitumor effect of the fusion toxin and was well tolerated, despite a longer circulation half-life<sup>11</sup> and thus a higher toxin exposure of the animals. Nonetheless, although such polymer attached to the DARPin part (which gets cleaved from the toxin by furin in



the endosome) can improve the pharmacokinetic properties of fusion toxins, it does not provide a mechanism for additional tumor-specific toxin activation.

In the present study, the advantage of bioorthogonal click chemistry was employed to generate DARPIn-ETA" fusion toxins site-specifically PEGylated at distinct positions in the toxin moiety. This approach was straightforward due to the lack of methionines in the sequence, enabling the introduction of unique ATG codons and thus unique Aha residues compatible with click chemistry by metabolic incorporation into *E. coli*. ETA" is very robust, and many single amino acid exchanges or insertions hardly affect its enzymatic activity.<sup>18–20,23,34</sup> Correspondingly, we found that most of the Aha mutations were well tolerated by the toxin without decreasing ribosylation inhibition activity in cell-free assays and cytotoxicity on tumor cells. By mutating the position behind the initiator codon to alanine to allow the *E. coli* methionine aminopeptidase to remove the N-terminal Aha, we could generate fusion toxins with only a single reactive azide for subsequent bioorthogonal PEGylation.

To avoid the negative effect of PEGylation on the therapeutic efficacy of ETA" fusion toxins, various strategies of reversible polymer conjugation were explored.<sup>23,25</sup> For instance, chemically unstable linker constructs between PEG and toxin have been described from which the polymer is slowly released over time.<sup>25,35</sup> This concept, however, relies on the assumption that the therapeutic window is determined by the balance between longer circulation times of intact PEGylated fusion toxin and faster renal clearance of spontaneously released uncoated toxin. Although this optimistic scenario may offer some improvement for tumor targeting, an additional layer of tumor-specificity is required. To address this issue, we engineered an activation mechanism which can in principle be triggered by proteases overexpressed in tumors. The use of protease cleavage sites has been widely reported in drug development.<sup>36–40</sup> For the same reason, a prodrug designed to focus the destructive power of ETA" to tumor cells upon reactivation by tumor proteases is more appealing than the sustained release concept, as it provides an additional step of specificity. The promising antitumor effect of our recently described N-terminally PEGylated anti-EpCAM fusion toxin<sup>11</sup> prompted us to generate such a prodrug-like fusion toxin by reversible PEGylation. Whereas PEGylation may help reducing the adverse effects of the toxin on normal tissues, the possibility of specific de-PEGylation by tumor proteases has the potential to increase tumor specificity further. For this reason, we conjugated PEG directly to the ETA" toxin using a linker construct containing the cleavage site for the highly specific rhinoviral 3C protease<sup>41</sup> as a model system. This approach is fully generic in nature, as the specificity of the peptide linker can in principle be adapted to any other protease known to be abundant in a given tumor type.

The intoxication process of ETA involves proteolytic cleavage by furin and reduction of an internal disulfide bridge. Thereby, the N-terminal part containing the targeting moiety is separated from the C-terminal fragment containing the catalytic domain, which then translocates into the cytosol.<sup>3</sup> Depending on the exact attachment site, PEG may interfere with any of these processes, as well as with the enzymatic activity itself, when it is attached within the catalytic domain and/or sequences responsible for the retrograde transport and/or the actual translocation step to the cytosol.

Conjugation of PEG to the catalytic domain of ETA was first reported by Benhar et al.,<sup>23</sup> albeit with different means and focus. The authors replaced a number of single surface-exposed residues in the catalytic domain of ETA by cysteine residues for site-specific modification with PEG to identify positions where the loss of activity was minimal. The toxin mutants were PEGylated irreversibly with 20 kDa PEG and the least active mutant (R490C) showed 23-fold loss of cytotoxicity. In contrast, we deliberately selected positions for PEG conjugation to achieve maximum loss of cytotoxicity upon PEGylation. Therefore, we picked residues close to the active site and the residues in contact with eEF2 or those likely involved in other crucial functions of the toxin such as retrograde transport from the endosome to the ER, mediated by the C-terminal KDEL motif. Interestingly, in contrast to previous reports<sup>23</sup> we found that PEGylation at these sites resulted in only marginally decreased cytotoxicity. The 47-fold decrease relative to the unPEGylated mutant toxin observed for PEGylated D574Aha was only twice as much as for the mutant R490C and hardly reversible by dePEGylation, presumably because the remaining stump still interfered with the enzymatic activity. The most pronounced reversible decrease was 30-fold and measured for Ec1-ETA"<sub>486Aha</sub>-3C-PEG. Although a direct comparison with the previously reported findings<sup>23</sup> is difficult due to different experimental setups, our data suggest that the measured loss of activity in our design is a consequence of interference with other intoxication steps rather than a direct inhibition of enzyme activity. This conclusion is supported by the finding that PEGylation in the catalytic domain hardly affected protein synthesis by ETA" in a cell-free system.

Reversible conjugation of a larger branched 40 kDa PEG at Aha486 in the catalytic domain resulted in an 80-fold increased IC<sub>50</sub> on HT29 cells, which was only about 3-fold more effective compared to a single linear 20 kDa PEG. On the other hand, we obtained a fusion toxin with nearly optimal prodrug-like behavior by dual-PEGylation at Aha486 and a second site upstream of the C-terminal KDEL peptide. PEGylation with two linear 20 kDa polymers resulted in a 15- to 25-fold higher loss of cytotoxicity measured on EpCAM-positive tumor cells, compared to mono-PEGylation at position 486 alone. Cytotoxicity was fully restored in the presence of 3C protease, and interestingly, the largest reactivation index of more than 1000-fold was determined on MDA-MB-231 cells, which express only very low levels of EpCAM. From the findings with low EpCAM-expressing target cells we conclude that the approach described here for reversible fusion toxin inactivation by designed PEGylation has the potential to reduce toxicity particularly also in normal epithelial tissues in which EpCAM is less abundant and which lack the protease required for prodrug activation.

Consistent with the favorable prodrug behavior, Ec1-ETA"<sub>486Aha</sub>-AhaKDEL-3C-PEG was much better tolerated in mice upon systemic administration, and despite a longer circulation half-life, caused only very marginal liver toxicity and weight loss compared to the unPEGylated fusion toxin. This suggests that our reversible polymer veiling strategy is a promising modality for increasing the therapeutic index of ETA". Moreover, we found that PEGylation also reduced the *in vitro* cytotoxicity of a nontargeted control fusion toxin, and in some cell lines the reactivation index was even higher than for the EpCAM-targeting toxins. This further suggests that a prodrug designed to become activated in the tumor, in this case by dePEGylation,



holds promise for sparing normal vital tissues from cytotoxic damage, independent of the cellular uptake mechanism.

Our data demonstrate that decreasing the systemic toxicity and increasing the maximum tolerated dose of DARPin-ETA<sup>+</sup> fusion toxins is possible by rational prodrug engineering using selected site-directed toxin mutagenesis and bioorthogonal click chemistry for reversible PEGylation. Further investigations are warranted to adapt the idea of fusion toxin engineering with a 3C protease-sensitive polymer veiling described here to a clinically relevant prodrug concept based on polymer linkage which is sensitive to tumor proteases or other enzymes delivered to the tumor by co-targeting.

## ■ EXPERIMENTAL PROCEDURES

**Materials.** If not otherwise stated, all reagents were obtained from Sigma-Aldrich (Buchs, Switzerland). *E. coli* strain B834 (DE3) ( $F^-$  *ompT gal hsdS<sub>B</sub> (r<sub>B</sub><sup>-</sup> m<sub>B</sub><sup>-</sup>) met dcm lon (lacI, lacUV5-T7 gene 1, ind1, sam7, nin5)*) was from EMD Chemicals, Inc. (U.S.A.) and *E. coli* strain XL1 blue (*recA1 endA1 gyrA96 thi-1 hsdR17 supE44 relA1 lac [F' proAB lacIqZΔM15 Tn10 (Tet<sup>r</sup>)]*) was purchased from Stratagene (Agilent Technologies, Inc., Santa Clara, CA, U.S.A.). Maleimido-*aza*-dibenzo-cyclooctyne (DBCO-maleimide) and DBCO-PEG<sub>20</sub> kDa were purchased from Click Chemistry Tools (Scottsdale, AZ, U.S.A.).

**Tumor Cell Cultures.** The EpCAM-positive carcinoma cell lines HT29, MCF-7, A431, MDA-MB-231, SKOV3, and SKBR3 were obtained from ATCC (American Type Culture Collection, LGC Standards S.à.r.l., Molsheim Cedex, France), MKN-45 cells were obtained from DSMZ (Deutsche Sammlung von Mikroorganismen und Zellkulturen GmbH, Braunschweig, Germany), MDA-MB-468 were obtained from CLS (Cell Lines Service GmbH, Eppelheim, Germany). HT29, A431, MDA-MB-468, and SKBR3 cells were grown in Dulbecco's modified Eagle medium (DMEM), MCF-7, MDA-MB-231, and SKOV3 cells were cultured in DMEM (50% v/v) and Ham's F12 medium (50% v/v), MKN-45 cells were grown in RPMI 1640. All media were supplemented with 10% (or 20% for MKN-45 cells) fetal calf serum (Amimed, Bioconcept, Allschwil, Switzerland), 100 units/mL penicillin, and 100 μg/mL streptomycin. Cells were incubated at 37 °C in a humidified atmosphere containing 5% CO<sub>2</sub>.

**Cloning. Removal of N-Terminal Amino Acid.** The codon following the start ATG of the coding sequence of Ec1-ETA<sup>+</sup> was mutated from AGA (Arg) to GCG (Ala), resulting in removal of N-terminal methionine or the non-natural amino acid azidohomoalanine (Aha).<sup>29</sup> In addition, to maintain translation initiation, the upstream ribosome binding site had to be adapted using the Web-based RBS calculator (<https://salis.psu.edu/software/>).<sup>42</sup> Briefly, a DNA fragment was synthesized by assembly PCR using oligonucleotides RBS<sub>r</sub> and MAGS<sub>f</sub> as template and RBS<sub>f</sub> and MAGS<sub>r</sub> as primers (Supporting Information Table S5). The resulting fragment was digested with *Eco*RI and *Bam*HI, and ligated into the expression vector pQIQ\_Ec1-ETA<sup>+</sup>,<sup>8,11</sup> cut with the same enzymes, yielding pQIQMA\_Ec1-ETA<sup>+</sup>. As an off-target control, a construct was prepared in which Ec1 was replaced by control DARPin Off7ΔM recognizing maltose binding protein.<sup>11</sup> Removal of the N-terminal Aha was confirmed by N-terminal sequencing.

**Introduction of ATG Codons into ETA<sup>+</sup> Domain III.** To identify suitable positions for replacement with Aha, the crystal structure (PDB: 2ZIT)<sup>30</sup> of ETA<sup>+</sup> domain III in complex with

eukaryotic elongation factor 2 (eEF2) and nicotinamide adenine dinucleotide (NAD<sup>+</sup>) was used as input for the protein interfaces, surfaces, and assemblies (PISA) server at the European Bioinformatics Institute (EBI).<sup>43</sup> The resulting map of interface residues was used to scan ETA<sup>+</sup> domain III for surface-exposed residues that are in proximity to the active site but not involved in direct contact with eEF2 or NAD<sup>+</sup>.

Single codon exchange for ATG within ETA<sup>+</sup> domain III as well as insertion of an ATG codon upstream of the C-terminal KDEL sequence was achieved by site-directed mutagenesis. Briefly, the plasmid pQIQMA\_Ec1-ETA<sup>+</sup> was amplified using primers listed in Supporting Information Table S5 followed by a *Dpn*I digest at 37 °C for 2 h. The mutated vector was transformed into chemo-competent *E. coli* XL1 blue cells and single colonies were used to inoculate overnight cultures. After sequencing, a positive clone was subcloned into the expression vector pQIQMA\_Ec1 backbone using *Hind*III and *Xba*I. The double mutant was generated by two sequential steps of site-directed mutagenesis as described above. The amino acid numbering system was based on mature wild-type ETA (UniProt: P11439). As an off-target control, DARPin Ec1 was replaced by Off7ΔM.<sup>11</sup>

**Expression and Purification of Clickable DARPin-Toxin Fusion Proteins.** The *E. coli* strain B834 (DE3) was transformed with the plasmid pQIQ encoding DARPin-ETA<sup>+</sup> or mutants thereof. A single colony was used to inoculate an overnight culture of 2 × YT medium supplemented with 100 μg/mL ampicillin and 1% glucose. On the next day, M9 minimal medium (SelenoMethionine Medium Base; Molecular Dimensions Ltd., Newmarket, United Kingdom) supplemented with 1% glucose, 50 mg/L ampicillin, a glucose-free nutrient mix containing 19 amino acids (Molecular Dimensions Ltd.), and 40 mg/L L-methionine was inoculated at an optical density at 600 nm (OD<sub>600</sub>) of 0.1 and grown in a shake flask at 37 °C until an OD<sub>600</sub> of 1.0–1.2 was reached. The culture was subsequently centrifuged (5000 × g, 15 min, 4 °C) and washed thoroughly by resuspension of the cell pellet in ice-cold 0.9% NaCl solution. The washing step was repeated twice on ice before resuspending the bacteria in M9 minimal medium (SelenoMethionine Medium Base; Molecular Dimensions Ltd.) supplemented with 0.4% glycerol, 50 mg/L ampicillin, a glucose-free nutrient mix containing 19 amino acids (Molecular Dimensions Ltd.), 50 mg/L ampicillin, and 40 mg/L L-azidohomoalanine (Aha) (Bapeks, Riga, Latvia). Cultures were shaken for 15 min at 30 °C and induced with 1 mM isopropyl-β-D-thio-galactopyranoside. After expression for 4 h at 30 °C, cultures were pelleted by centrifugation (15 min, 5000 × g, 4 °C), the pellet was washed with 0.9% NaCl and stored overnight at –80 °C. For protein purification, the bacteria were resuspended in TBS<sub>400</sub> (50 mM Tris, 400 mM NaCl, pH 7.4, at 4 °C) with 20 mM imidazole and lysed by sonication (Sonifier 250, Branson, 3 cycles on ice, duty cycle 50%, output control 5) or by using a French press (Aminco, 2 passages, 1200 psi). After centrifugation (48 000 × g, 30 min, 4 °C) and filtration (pore size 0.22 μm), the fusion toxin present in the clear supernatant was purified by immobilized metal ion affinity chromatography (IMAC) using Ni-NTA Superflow (Qiagen). The pooled elution fractions were diluted 10-fold in AEC buffer A (20 mM Tris, 20 mM NaCl, pH 8.0), loaded on a MonoQ column connected to an Äkta Explorer FPLC device (GE Healthcare Europe GmbH, Switzerland), and eluted with a gradient from 0% to 50% AEC buffer B (20 mM Tris, 1 M NaCl, pH 8.0). The fractions containing the fusion toxin were

pooled and concentrated (Amicon Ultra-4 Centrifugal Filter Unit, MWCO 30 kDa, Millipore AG, Zug, Switzerland) according to the manufacturer's protocol in PBS supplemented with 10% glycerol. Concentrations were determined by UV absorbance at 280 nm using a NanoDrop 1000 (Thermo Scientific AG, Wohlen, Switzerland).

**N-Terminal Sequencing.** Removal of the N-terminal non-natural amino acid Aha was verified using N-terminal protein sequencing. A volume of 2  $\mu$ L Ec1-ETA<sup>486Aha</sup> (approximately 5  $\mu$ g) was diluted in 100  $\mu$ L 0.1% trifluoroacetic acid (TFA) and loaded on a Prosorb Sample Preparation Cartridge (ABI). The membrane was washed twice with 0.1% TFA before Edman degradation was performed using a PROCISE cLC492 system to determine N-terminal amino acid residues.

**Synthesis and Purification of PEG-3C-DBCO and Y-PEG-3C-DBCO.** One milligram (772 pmol) of the 3C protease-cleavable peptide SDSLEVLFGGPC (United Biosystems Inc., Herndon, VA, U.S.A.) was dissolved in 50  $\mu$ L 25 mM NaOH and diluted to 772  $\mu$ M with 950  $\mu$ L 20 mM HEPES, pH 7.7. Two equivalents DBCO-maleimide (Click Chemistry Tools) dissolved in dimethylformamide was added and the mixture was incubated at 25 °C for 30 min under vigorous shaking. Thereafter, 4.3 equiv mPEG-succinimidyl valerate MW 20 kDa (66 mg mPEG-SVA-20K; LaysanBio Inc., Arab, AL, U.S.A.) or branched PEG NHS Ester MW 40 kDa (133 mg Y-NHS-40K; JenKem Technology USA Inc., Allen, TX, U.S.A.) were added, the reaction was diluted with 300  $\mu$ L 100 mM HEPES, pH 8.75, and shaken at 25 °C for another 2 h. For quenching, 10 mM Tris and 10 mM 2-mercaptoethanol was added and allowed to react for 30 min before removing low MW components by a PD-10 desalting column (GE Healthcare) equilibrated with H<sub>2</sub>O. Unreacted PEG was removed by anion exchange chromatography using a 5 mL DEAE Sepharose FF column (GE Healthcare). The desalted reaction mix was loaded on the column equilibrated with H<sub>2</sub>O and the desired product PEG-3C-DBCO or Y-PEG-3C-DBCO was eluted with a gradient from 0 to 0.5 M NaCl. Fractions were analyzed by native PAGE on 8% polyacrylamide gels and PEG was visualized by barium iodide staining.<sup>31</sup> Briefly, gels were fixed, washed with water, incubated for 15 min in 20 mL 0.1 M perchloric acid before adding 5 mL 5% BaCl<sub>2</sub> and 2 mL 0.1 M iodine solution. After another desalting step, PEG-3C-DBCO or Y-PEG-3C-DBCO was quantified by measuring the characteristic absorbance of DBCO at 309 nm (molar extinction coefficient = 12 000 M<sup>-1</sup> cm<sup>-1</sup>), lyophilized overnight in a freeze-dryer (Brouwer, Rotkreuz, Switzerland), and stored at -20 °C.

**Cu-Free Click PEGylation and Purification.** The different variants of Ec1-ETA<sup>486Aha</sup> were reacted at 44–100  $\mu$ M concentrations with a 3-fold molar excess of 3C-cleavable PEG-3C-DBCO, Y-PEG-3C-DBCO, or commercially available non-cleavable PEG-DBCO (Click Chemistry Tools) at 4 °C for 48 h under constant slow rotation. PEGylated Ec1-ETA<sup>486Aha</sup> was separated from unreacted PEGylation reagent and from non-PEGylated Ec1-ETA<sup>486Aha</sup> by anion exchange chromatography using a MonoQ GL 5/50 column. The reaction mix was diluted in AEC buffer A (see above), loaded on the MonoQ column, and eluted with a gradient from 0% to 50% AEC buffer B. The fractions containing PEGylated Ec1-ETA<sup>486Aha</sup> were pooled, concentrated (Amicon Ultra-4 Centrifugal Filter Unit, MWCO 30 kDa, Millipore), and run on a Superdex 200 10/300 GL gel filtration column (GE Healthcare) equilibrated with PBS, pH 7.4. The fractions containing monomeric PEGylated

Ec1-ETA<sup>486Aha</sup> were pooled, concentrated (Amicon Ultra-4 Centrifugal Filter Unit, MWCO 30 kDa, Millipore) in PBS supplemented with 10% glycerol, and stored at -80 °C until use. Concentrations were determined by UV absorbance at 280 nm using a NanoDrop 1000 (Thermo Scientific, Switzerland). Purity was assessed on 12% SDS-polyacrylamide gels, Coomassie-stained for protein, and barium iodide-stained for PEG as described above.

**Proteolytic PEG Removal.** PEGylated DARPIn-ETA<sup>486Aha</sup> variants were incubated for 2 h on ice with 0.01 equiv human rhinovirus 3C protease produced in-house by recombinant expression in *E. coli* and IMAC purification. Efficiency of PEG removal was assessed by SDS-PAGE and staining for protein and PEG as described above.

**Analytical Gel Filtration.** Unmodified and PEGylated proteins were evaluated by analytical gel filtration using a Superdex 200 PC3.2/30 column in combination with an Akta Micro FPLC (GE Healthcare Europe GmbH, Switzerland). Degassed and sterile filtered PBS pH 7.4 was used as running buffer. A standard containing  $\beta$ -amylase (200 kDa), BSA (66 kDa), carbonic anhydrase (29 kDa), and cytochrome *c* (12.4 kDa) was used to calculate the apparent molecular weights ( $M_{w,app}$ ) of the products.

**Translation Inhibition Assay.** The catalytic activities of the unPEGylated, PEGylated, and dePEGylated Ec1-ETA<sup>486Aha</sup> variants were determined by monitoring the concentration-dependent inhibition of an *in vitro* translation reaction. A dilution series of the toxins ranging 100 nM to 10 pM was incubated for 15 min at 30 °C with a rabbit reticulocyte lysate-based translation mix (Promega, Madison, WI, U.S.A.) supplemented with 100  $\mu$ M NAD<sup>+</sup>. Translation was started by adding 1  $\mu$ g RNA encoding *Renilla* luciferase and allowed to proceed for 90 min at 30 °C before adding 0.2 mg/mL RNase A (Macherey-Nagel). Translated *Renilla* luciferase was quantified on a GloMax-Multi instrument (Promega) using the *Renilla* Luciferase Assay Kit (Biotium, Hayward, CA, U.S.A.) according to the manufacturer's instructions. Values were normalized to translation reactions without inhibitor and fit to a 4-parameter sigmoidal equation with variable slope using the Prism program (v. 6.00, GraphPad Software, San Diego, CA, U.S.A.) to calculate the concentration of toxin at which translation was inhibited by 50% (IC<sub>50</sub>). Statistical significance was calculated using two-way ANOVA with Tukey post-test.

**Affinity Measurements.** The EpCAM-binding affinity of the unmodified and PEGylated Ec1-ETA<sup>486Aha</sup> toxins was measured by surface plasmon resonance using a ProteOn XPR36 (Bio-Rad Laboratories, Hercules, U.S.A.). Two ligand channels of a Neutravidin Sensor Chip (NLC) were coated with 1000 resonance units of the extracellular domain of EpCAM (residues 1–242 of the mature protein) biotinylated using an AviTag. Kinetic data were obtained by parallel injection of different toxins at concentrations ranging from 1 to 100 nM at a buffer flow rate of 60  $\mu$ L/min in PBS, pH 7.4, containing 3 mM EDTA and 0.005% Tween-20. Two short pulses of 100 mM H<sub>3</sub>PO<sub>4</sub>, pH 1.75 were used for regeneration. Data were analyzed using the ProteOn Manager software (Bio-Rad Laboratories).

**Cytotoxicity Assays.** The cytotoxicity of unPEGylated, PEGylated, and dePEGylated DARPIn-ETA<sup>486Aha</sup> variants was assessed by measuring cell viability in standard colorimetric XTT assays (Cell Proliferation Kit II; Roche Diagnostics AG, Rotkreuz, Switzerland). Briefly, 2000–5000 EpCAM-positive tumor cells per well were seeded in a 96-well plate and

incubated for 24 h at 37 °C under standard cell culture conditions as described above. The fusion proteins were added to the cells at the indicated concentrations to a final volume of 100  $\mu$ L. After 72 h, medium was removed by decanting, and 50  $\mu$ L of XTT reagent was added as specified by the manufacturer's protocol, and cells were incubated for another 2 h. The absorbance at 480 nm minus that at 650 nm was measured with an Infinite M1000 microplate reader (Tecan Group Ltd., Männedorf, Switzerland). Cell viability was calculated after subtraction of the value of dead cells (wells with cells treated with 1 mg/mL Hygromycin B) and presented as the percentage of viable cells in the treated wells relative to untreated cells (cells without DARPIn-ETA<sup>n</sup>). Data were fit to a three-parameter sigmoidal equation using the Prism program (v 6.00, GraphPad Software, San Diego, CA, U.S.A.) to calculate the concentration of toxin at which cell viability was reduced by 50% (IC<sub>50</sub>).

For competition analysis of specificity, cells were first incubated for 30 min with 10  $\mu$ M unconjugated DARPIn Ec1 before Ec1-ETA<sup>n</sup> variants were added and cell viability was determined.

#### Pharmacokinetic and Toxicity Analyses in Mice.

Female C57BL/6 mice (8 weeks of age) were obtained from Charles River (Sulzfeld, Germany). Mice were injected into the lateral tail vein with 20 nmol/kg body weight of either Ec1-ETA<sup>n</sup> ( $n = 4$ ) or Ec1-ETA<sup>n</sup><sub>486Aha-AhaKDEL</sub>-3C-PEG ( $n = 3$ ). Blood samples were drawn from the tail vein at various time points: for Ec1-ETA<sup>n</sup> at 3, 15, 30, 45, 75, and 120 min and for Ec1-ETA<sup>n</sup><sub>486Aha-AhaKDEL</sub>-3C-PEG at 3 min and 1, 3, 6, 9, 12, and 24 h post injection. The blood was left to coagulate at room temperature (RT) for 30 min and the serum was separated by two centrifugation steps (7 min, 3000  $\times$  g at RT) and stored at -20 °C until analysis of serum concentrations of the drug conjugates by enzyme-linked immunosorbent assay (ELISA). In brief, MaxiSorp 96-well plates (Nunc GmbH & Co. KG, Langenselbold, Germany) were coated with mouse anti-tetra-His antibody (Qiagen) at a dilution of 1:2000 for Ec1-ETA<sup>n</sup> and at a dilution of 1:1000 for Ec1-ETA<sup>n</sup><sub>486Aha-AhaKDEL</sub>-3C-PEG in PBS at 4 °C overnight. The wells were blocked with 300  $\mu$ L PBS-TB (PBS, 0.2% BSA, 0.1% Tween-20) for 1 h at RT. Serum samples were diluted to the range of the standard curve in PBS-TB and applied in duplicate to the coated wells. Serum of a control mouse that did not receive any injection was diluted accordingly and analyzed for background signals. For quantification, a serial dilution of Ec1-ETA<sup>n</sup> and Ec1-ETA<sup>n</sup><sub>486Aha-AhaKDEL</sub>-3C-PEG ranging from 0.05 nM to 2 nM were included on each plate. Samples were incubated for 1 h at room temperature. After stringent washes with PBS-T (PBS, 0.1% Tween-20), anti-PE polyclonal serum (Sigma-Aldrich) was added as primary antibody at a dilution of 1:5000 in PBS-TB for 1 h at RT. Washing with PBS-T was followed by incubation with the secondary antibody (goat-anti-rabbit IgG-HRP conjugate, Sigma-Aldrich) at a dilution of 1:10 000 in PBS-TB for 1 h at RT. After four wash steps with PBS-T, the assay was developed using Amplex UltraRed Reagent (Invitrogen, Life Technologies, Europe B.V., Zug, Switzerland) diluted in PBS at a 2-fold lower concentration than recommended by the manufacturer. Fluorescence was measured with an Infinite M1000 microplate reader (Tecan Group Ltd., Männedorf, Switzerland) with excitation at 490 nm and emission at 585 nm. A four-parameter logistic regression model was used to fit the data points from the serial dilution using the software R (v. 3.1.1) and the R package drc (v. 2–3.96). The so

obtained standard curve was used to calculate the Ec1-ETA<sup>n</sup> and Ec1-ETA<sup>n</sup><sub>486Aha-AhaKDEL</sub>-3C-PEG concentrations of the serum samples. The area under the curves was calculated using the Prism program (v 6.00, GraphPad Software, San Diego, CA, U.S.A.).

For toxicity analyses, female C57BL/6 mice (8 weeks of age) were injected into the lateral tail vein with 1 or 2.5 mg/kg bodyweight of Ec1-ETA<sup>n</sup> or 1, 2.5, or 7.5 mg/kg bodyweight of Ec1-ETA<sup>n</sup><sub>486Aha-AhaKDEL</sub>-3C-PEG. Body weight and behavior of mice were recorded for 72 h. After 72 h, mice were sacrificed and blood was harvested by heart puncture for analysis of transaminases. Blood serum was obtained by two centrifugation steps (7 min, 3000  $\times$  g at RT). The serum was analyzed for AST and ALT the same day at the Institute of Clinical Chemistry at University Hospital of Zurich according to an IFCC (International Federation of Clinical Chemistry and Laboratory Medicine) standardized photometric method with pyridoxal phosphate activation. Statistical significance was determined by one-way analysis of variance (ANOVA) with Sidak's multiple comparison test using the Prism program (v 6.00, GraphPad Software, San Diego, CA, U.S.A.).

## ■ ASSOCIATED CONTENT

### ■ Supporting Information

Figures S1–S3 and Tables S1–S5. This material is available free of charge via the Internet at <http://pubs.acs.org>.

## ■ AUTHOR INFORMATION

### Corresponding Authors

\*E-mail: [uwe.zangemeister@pki.unibe.ch](mailto:uwe.zangemeister@pki.unibe.ch), Phone: +41-31-632 3290, Fax: +41-31-632 4992.

\*E-mail: [plueckthun@bioc.uzh.ch](mailto:plueckthun@bioc.uzh.ch), Phone: +41-44-635-5570, Fax: +41-44-635-5712.

### Present Address

Nikolas Stefan, NBE Therapeutics LLC, Technology Park Basel, Basel, Switzerland. Manuel Simon, Discovery Oncology, Roche Pharma Research and Early Development (pRED), Roche Innovation Center Penzberg, Germany.

### Notes

The authors declare the following competing financial interest(s): A. Plückthun is a shareholder of Molecular Partners AG, which is commercializing the DARPIn technology. The other authors disclosed no potential conflicts of interest.

## ■ ACKNOWLEDGMENTS

This work was supported by Swiss National Science Foundation grants 310030\_119859 and 31003A\_138201.

## ■ REFERENCES

- (1) FitzGerald, D. J., Wayne, A. S., Kreitman, R. J., and Pastan, I. (2011) Treatment of hematologic malignancies with immunotoxins and antibody-drug conjugates. *Cancer Res.* 71, 6300–9.
- (2) Pastan, I., Hassan, R., Fitzgerald, D. J., and Kreitman, R. J. (2006) Immunotoxin therapy of cancer. *Nat. Rev. Cancer* 6, 559–65.
- (3) Weldon, J. E., and Pastan, I. (2011) A guide to taming a toxin - recombinant immunotoxins constructed from *Pseudomonas* exotoxin A for the treatment of cancer. *FEBS J.* 278, 4683–4700.
- (4) Simon, M., Stefan, N., Plückthun, A., and Zangemeister-Wittke, U. (2013) Epithelial cell adhesion molecule-targeted drug delivery for cancer therapy. *Expert Opin. Drug Delivery* 10, 451–68.
- (5) Martin-Killias, P., Stefan, N., Rothschild, S., Plückthun, A., and Zangemeister-Wittke, U. (2011) A novel fusion toxin derived from an



EpCAM-specific designed ankyrin repeat protein has potent antitumor activity. *Clin. Cancer. Res.* 17, 100–110.

(6) Boersma, Y. L., and Plückthun, A. (2011) DARPin and other repeat protein scaffolds: advances in engineering and applications. *Curr. Opin. Biotechnol.* 22, 849–857.

(7) Binz, H. K., Stumpp, M. T., Forrer, P., Amstutz, P., and Plückthun, A. (2003) Designing repeat proteins: well-expressed, soluble and stable proteins from combinatorial libraries of consensus ankyrin repeat proteins. *J. Mol. Biol.* 332, 489–503.

(8) Simon, M., Zangemeister-Wittke, U., and Plückthun, A. (2012) Facile double-functionalization of Designed Ankyrin Repeat Proteins using click and thiol chemistries. *Bioconjugate Chem.* 23, 279–286.

(9) Spizzo, G., Fong, D., Wurm, M., Ensinger, C., Obrist, P., Hofer, C., Mazzoleni, G., Gastl, G., and Went, P. (2011) EpCAM expression in primary tumour tissues and metastases: an immunohistochemical analysis. *J. Clin. Pathol.* 64, 415–20.

(10) Went, P., Lugli, A., Meier, S., Bundi, M., Mirlacher, M., Sauter, G., and Dirnhofer, S. (2004) Frequent EpCAM protein expression in human carcinomas. *Hum. Pathol.* 35, 122–128.

(11) Simon, M., Stefan, N., Borsig, L., Plückthun, A., and Zangemeister-Wittke, U. (2014) Increasing the antitumor effect of an EpCAM-targeting fusion toxin by facile click PEGylation. *Mol. Cancer Ther.* 13, 375–85.

(12) Hassan, R., Bullock, S., Premkumar, A., Kreitman, R. J., Kindler, H., Willingham, M. C., and Pastan, I. (2007) Phase I study of SS1P, a recombinant anti-mesothelin immunotoxin given as a bolus i.v. infusion to patients with mesothelin-expressing mesothelioma, ovarian, and pancreatic cancers. *Clin. Cancer. Res.* 13, 5144–9.

(13) Schümann, J., Angermüller, S., Bang, R., Lohoff, M., and Tiegs, G. (1998) Acute hepatotoxicity of *Pseudomonas aeruginosa* exotoxin A in mice depends on T cells and TNF. *J. Immunol.* 161, 5745–54.

(14) Kreitman, R. J., Wilson, W. H., Bergeron, K., Raggio, M., Stetler-Stevenson, M., FitzGerald, D. J., and Pastan, I. (2001) Efficacy of the anti-CD22 recombinant immunotoxin BL22 in chemotherapy-resistant hairy-cell leukemia. *New Engl. J. Med.* 345, 241–7.

(15) Kreitman, R. J., and Pastan, I. (1995) Importance of the glutamate residue of KDEL in increasing the cytotoxicity of *Pseudomonas* exotoxin derivatives and for increased binding to the KDEL receptor. *Biochem. J.* 307 (Pt 1), 29–37.

(16) Weldon, J. E., Xiang, L., Chertov, O., Margulies, I., Kreitman, R. J., FitzGerald, D. J., and Pastan, I. (2009) A protease-resistant immunotoxin against CD22 with greatly increased activity against CLL and diminished animal toxicity. *Blood* 113, 3792–800.

(17) Weldon, J. E., Xiang, L., Zhang, J., Beers, R., Walker, D. A., Onda, M., Hassan, R., and Pastan, I. (2013) A recombinant immunotoxin against the tumor-associated antigen mesothelin reengineered for high activity, low off-target toxicity, and reduced antigenicity. *Mol. Cancer Ther.* 12, 48–57.

(18) Onda, M., Beers, R., Xiang, L., Lee, B., Weldon, J. E., Kreitman, R. J., and Pastan, I. (2011) Recombinant immunotoxin against B-cell malignancies with no immunogenicity in mice by removal of B-cell epitopes. *Proc. Natl. Acad. Sci. U.S.A.* 108, 5742–7.

(19) Mazor, R., Vassall, A. N., Eberle, J. A., Beers, R., Weldon, J. E., Venzon, D. J., Tsang, K. Y., Benhar, I., and Pastan, I. (2012) Identification and elimination of an immunodominant T-cell epitope in recombinant immunotoxins based on *Pseudomonas* exotoxin A. *Proc. Natl. Acad. Sci. U.S.A.* 109, E3597–603.

(20) Onda, M., Nagata, S., FitzGerald, D. J., Beers, R., Fisher, R. J., Vincent, J. J., Lee, B., Nakamura, M., Hwang, J., Kreitman, R. J., Hassan, R., and Pastan, I. (2006) Characterization of the B cell epitopes associated with a truncated form of *Pseudomonas* exotoxin (PE38) used to make immunotoxins for the treatment of cancer patients. *J. Immunol.* 177, 8822–34.

(21) Alconcel, S. N. S., Baas, A. S., and Maynard, H. D. (2011) FDA-approved poly(ethylene glycol)–protein conjugate drugs. *Polym. Chem.* 2, 1442.

(22) Veronese, F. M., and Pasut, G. (2005) PEGylation, successful approach to drug delivery. *Drug Discovery Today* 10, 1451–1458.

(23) Benhar, I., Wang, Q. C., Fitzgerald, D., and Pastan, I. (1994) *Pseudomonas* exotoxin-a mutants - replacement of surface-exposed residues in domain-III with cysteine residues that can be modified with polyethylene-glycol in a site-specific manner. *J. Biol. Chem.* 269, 13398–13404.

(24) Tsutsumi, Y., Onda, M., Nagata, S., Lee, B., Kreitman, R. J., and Pastan, I. (2000) Site-specific chemical modification with polyethylene glycol of recombinant immunotoxin anti-Tac(Fv)-PE38 (LMB-2) improves antitumor activity and reduces animal toxicity and immunogenicity. *Proc. Natl. Acad. Sci. U.S.A.* 97, 8548–8553.

(25) Filpula, D., Yang, K., Basu, A., Hassan, R., Xiang, L., Zhang, Z., Wang, M., Wang, Q. C., Ho, M., Beers, R., Zhao, H., Peng, P., Zhou, J., Li, X., Petti, G., Janjua, A., Liu, J., Wu, D., Yu, D., Zhang, Z., Longley, C., FitzGerald, D., Kreitman, R. J., and Pastan, I. (2007) Releasable PEGylation of mesothelin targeted immunotoxin SS1P achieves single dosage complete regression of a human carcinoma in mice. *Bioconjugate Chem.* 18, 773–84.

(26) Harris, J. M., and Chess, R. B. (2003) Effect of PEGylation on pharmaceuticals. *Nat. Rev. Drug Discovery* 2, 214–21.

(27) Bailon, P., and Won, C. Y. (2009) PEG-modified biopharmaceuticals. *Expert Opin. Drug Delivery* 6, 1–16.

(28) Stefan, N., Martin-Killias, P., Wyss-Stoeckle, S., Honegger, A., Zangemeister-Wittke, U., and Plückthun, A. (2011) DARPin recognizing the tumor-associated antigen EpCAM selected by phage and ribosome display and engineered for multivalency. *J. Mol. Biol.* 413, 826–843.

(29) Wang, A., Winblade Nairn, N., Johnson, R. S., Tirrell, D. A., and Grabstein, K. (2008) Processing of N-terminal unnatural amino acids in recombinant human interferon-beta in *Escherichia coli*. *Chem-BioChem* 9, 324–330.

(30) Jorgensen, R., Wang, Y., Visschedyk, D., and Merrill, A. R. (2008) The nature and character of the transition state for the ADP-ribosyltransferase reaction. *EMBO Rep.* 9, 802–9.

(31) Kurfürst, M. M. (1992) Detection and molecular weight determination of polyethylene glycol-modified hirudin by staining after sodium dodecyl sulfate-polyacrylamide gel electrophoresis. *Anal. Biochem.* 200, 244–248.

(32) Kubetzko, S., Sarkar, C. A., and Plückthun, A. (2005) Protein PEGylation decreases observed target association rates via a dual blocking mechanism. *Mol. Pharmacol.* 68, 1439–1454.

(33) Wang, Q. C., Pai, L. H., Debinski, W., FitzGerald, D. J., and Pastan, I. (1993) Polyethylene glycol-modified chimeric toxin composed of transforming growth factor alpha and *Pseudomonas* exotoxin. *Cancer Res.* 53, 4588–94.

(34) Liu, W., Onda, M., Lee, B., Kreitman, R. J., Hassan, R., Xiang, L., and Pastan, I. (2012) Recombinant immunotoxin engineered for low immunogenicity and antigenicity by identifying and silencing human B-cell epitopes. *Proc. Natl. Acad. Sci. U.S.A.* 109, 11782–7.

(35) Tsubery, H., Mironchik, M., Fridkin, M., and Shechter, Y. (2004) Prolonging the action of protein and peptide drugs by a novel approach of reversible polyethylene glycol modification. *J. Biol. Chem.* 279, 38118–24.

(36) Olson, E. S., Jiang, T., Aguilera, T. A., Nguyen, Q. T., Ellies, L. G., Scadeng, M., and Tsien, R. Y. (2010) Activatable cell penetrating peptides linked to nanoparticles as dual probes for in vivo fluorescence and MR imaging of proteases. *Proc. Natl. Acad. Sci. U.S.A.* 107, 4311–6.

(37) Jiang, T., Olson, E. S., Nguyen, Q. T., Roy, M., Jennings, P. A., and Tsien, R. Y. (2004) Tumor imaging by means of proteolytic activation of cell-penetrating peptides. *Proc. Natl. Acad. Sci. U.S.A.* 101, 17867–72.

(38) Terada, T., Iwai, M., Kawakami, S., Yamashita, F., and Hashida, M. (2006) Novel PEG-matrix metalloproteinase-2 cleavable peptide-lipid containing galactosylated liposomes for hepatocellular carcinoma-selective targeting. *J. Controlled Release* 111, 333–42.

(39) Harris, T. J., von Maltzahn, G., Lord, M. E., Park, J. H., Agrawal, A., Min, D. H., Sailor, M. J., and Bhatia, S. N. (2008) Protease-triggered unveiling of bioactive nanoparticles. *Small* 4, 1307–12.

- (40) Hatakeyama, H., Akita, H., Kogure, K., Oishi, M., Nagasaki, Y., Kihira, Y., Ueno, M., Kobayashi, H., Kikuchi, H., and Harashima, H. (2007) Development of a novel systemic gene delivery system for cancer therapy with a tumor-specific cleavable PEG-lipid. *Gene Ther.* 14, 68–77.
- (41) Malcolm, B. A. (1995) The picornaviral 3C proteinases: cysteine nucleophiles in serine proteinase folds. *Protein Sci.* 4, 1439–45.
- (42) Salis, H. M., Mirsky, E. A., and Voigt, C. A. (2009) Automated design of synthetic ribosome binding sites to control protein expression. *Nat. Biotechnol.* 27, 946–50.
- (43) Krissinel, E., and Henrick, K. (2007) Inference of macromolecular assemblies from crystalline state. *J. Mol. Biol.* 372, 774–97.